

Intense electron beam propagation through insulators: ionization front corrugation and ionization instabilities

S. I. Krasheninnikov¹, A. V. Kim², B. K. Frolov¹, and R. B. Stephens³

¹University of California at San Diego, La Jolla, CA, USA

²Institute of Applied Physics RAS, Nizhny Novgorod, Russia

³General Atomics, San Diego, CA, USA

I. Introduction. Recently it was found [1] that the energetic proton beams are generated during the interactions of intense electron beams with the foils. However, it appears that the homogeneity of the electron and, therefore, proton beams depend on the material of the foil. It was shown that for conductive material electron beam is rather homogeneous, while in the case of insulators it exhibits strongly filamentary structure [2, 3]. Here we consider the propagation of intense electron beam through an insulator and focus on: i) self-consistent structure of 1D ionization front and the impact of the electric field ionization processes [4], and ii) the linear instabilities of the front, which may result in the beam filamentarization (more details can be found in Ref. 5).

II. Equations. We consider the processes of ionization of insulator by both beam and secondary electrons as well as by the electric field effects. In the frame of the front we have the following equations describing the evolution of secondary electron, n_e , and ion, n_i , densities

$$\partial n_i / \partial t + \nabla \cdot (\mathbf{V}_f n_i) = \nu_{EI}(\mathbf{E}) N_a + \nu_{bI} n_b + \nu_{eI} n_e, \quad (1)$$

$$\partial n_e / \partial t + \nabla \cdot \{(\mathbf{V}_f + \mathbf{V}_e) n_e\} = \nu_{EI}(\mathbf{E}) N_a + \nu_{bI} n_b + \nu_{eI} n_e, \quad (2)$$

where n_b is the beam density; N_a is the density of atoms in the insulator; $\mathbf{V}_f = e_x V_f$ is the velocity of the ionization front; e_x is the unit vector along the x-coordinate; \mathbf{V}_e is the electron drift velocity ($|\mathbf{V}_e| \ll V_f$); $\nu_{EI}(\mathbf{E})$, ν_{bI} , and ν_{eI} are the ionization frequencies by the electric field effects, and by the beam and secondary electrons respectively. In Eq. (1) we assume that the ions are immobile and that $\nu_{bI} = K_{bI} N_a$ and $\nu_{eI} = K_{eI} N_a$, where K_{bI} and K_{eI} are constants, and the electron drift velocity and the electric field ionization frequency are given by the following expressions

$$\mathbf{V}_e + \mathbf{V}_f = -e\mathbf{E} / \gamma_f m v_e - (e / \gamma_f m c v_e) (\mathbf{V}_e + \mathbf{V}_f) \times \mathbf{B}, \quad \nu_{EI}(\mathbf{E}) = \nu_a E_a / |\mathbf{E}| \exp(-E_a / |\mathbf{E}|), \quad (3)$$

where e and m are the electric charge and mass of the electron; c is the light speed; $\gamma_f^{-2} = 1 - (V_f/c)^2$; $\nu_e \equiv K_e N_a$ is the collision frequency of secondary electrons with the atoms of the insulator; $\nu_a = 6m e^4 / \hbar^3$; E_a is the atomic electric field. We neglect the change of atom density in the insulator because when plasma density becomes of the order of atom density, the electric field is so small that it practically does not affect the beam propagation. In addition to the equations (1) and (2) we also need to consider the Maxwell equations and the beam dynamics. For the steady state case in the front frame the beam density is the function of the electrostatic potential φ , $n_b = n_b(\varphi)$. In our study we choose

$$n_b(\varphi) = \bar{n}_b (e\varphi / W_b)^p, \quad (4)$$

where W_b is the maximum energy of the beam electrons in the front frame, \bar{n}_b is the density of the beam far away from the front where the electric field is small, and p is an adjustable parameter. We assume here that the electrostatic potential is approaching zero before the ionization front and reaches $\varphi_b = W_b / e$ at the source of the beam.

III. Structure of the 1D ionization front. For the 1D ionization front there are only x-components of electric field and electron velocity $V_e = -eE / \gamma_f m v_e \equiv V_E$. For $V_E \ll V_f$ we

simplify the equation for the secondary electron density $\delta n \equiv n_i - n_e = (V_E/V_f)n_i$ and arrive to the Poisson equation $dE/dx = -4\pi e(n_b(\phi) - \delta n)$. Introducing dimensionless variables: $\phi = e\varphi/W_b$ ($0 \leq \phi \leq 1$, where $\phi = 0$ corresponds to the “head” of the beam), $\varepsilon = -E/E_a$, $\hat{n}_i = (V_{E_a}/V_f)(n_i/\bar{n}_b)$, where $V_{E_a} \equiv \bar{V}_{E_a}/\gamma_f = eE_a/(\gamma_f m v_e)$ and changing derivatives $d(\dots)/dx$ to $(E_a/eW_b)\varepsilon d(\dots)/d\phi$, from Eqs. (1), (8-11) we write the Poisson and ion density continuity equations as follows

$$d\varepsilon/d\phi = C_{bE}(\phi^p/\varepsilon - \hat{n}_i), \quad \varepsilon(d\hat{n}_i/d\phi) = \hat{v}_{EI}(\varepsilon) + \hat{v}_{bI}\phi^p + \hat{v}_{eI}\hat{n}_i, \quad (5)$$

where $\hat{v}_{bI} = C_{bf}(v_{bI}/v_e)$, $\hat{v}_{eI} = C_{bf}(v_{eI}/v_e)(V_f/V_{E_a})$, $\hat{v}_{EI}(\varepsilon) = C_{bf}(v_{EI}(\varepsilon)/v_e)(N_a/\bar{n}_b)$, $C_{bf} = W_b/\gamma_f m V_f^2$, and $C_{bE} = 4\pi W_b \bar{n}_b/E_a^2$. Solving Eqs. (5) with the “natural” boundary conditions $\varepsilon(\phi=0) = \hat{n}_i(\phi=0) = \varepsilon(\phi=1) = 0$ we find both the profiles of the electrostatic potential and plasma density as well as the velocity of the ionization front. However, the analysis of these equations at $\phi \rightarrow 0$ shows that such boundary conditions can only be satisfied for $0 < p \leq 1$, giving $\phi(x) \propto x^{2/(1-p)}$, at $\phi \rightarrow 0$. Next, from Eq. (5) we find that the value of ε is limited by the inequality $\varepsilon \lesssim C_{bE}^{1/2} \equiv (4\pi W_b \bar{n}_b/E_a^2)^{1/2}$. Then, recalling $v_{EI} \propto \exp(-1/\varepsilon)$, we conclude that the field ionization starts to be important only for high beam energy density, $C_{bE} \gtrsim 10^{-2}$, which roughly corresponds to $\varepsilon \gtrsim 0.1$, since otherwise v_{EI} becomes exponentially small.

For $p \ll 1$ we solve Eq. (5) analytically and find that at high beam energy density the electric field ionization occurs in a very vicinity, $\delta x_{EI} \sim x_m \sqrt{\varepsilon_m} \ll x_m$, around the maximum values of the electric field, ε_m , which is determined by the relation

$$\varepsilon_m^3 (E_a^2/8\gamma_f m V_f^2 \bar{n}_b)(N_a/\bar{n}_b)(v_{EI}(\varepsilon_m)/v_e) = 1, \quad (6)$$

and is located at $x = x_m \equiv \varepsilon_m E_a/4\pi e \bar{n}_b$. We also find a non-monotonic dependence of the ionization front on the beam density caused by the electric field ionization effects and which can be explained as follows. For a small beam density the ionization is only due to binary collisions. Therefore, the width of the electron impact ionization region can be estimated as $\Delta_{e-ion} \sim V_f/v_{eI}$. Then from the Poisson equation and the beam energy balance we have $E/\Delta_{e-ion} \sim 4\pi e n_b$ and $eE\Delta_{e-ion} \sim W_b$ which give the estimates for both front velocity and the electric field strength

$$V_f \sim v_{eI} \sqrt{W_b/4\pi e^2 n_b}, \quad E^2 \sim 4\pi W_b n_b. \quad (7)$$

With an increase of beam energy density, the electric field increases (see Eq. (7)) and finally we need to account for the electric field ionization processes. In this case a) the maximum of the electric field is limited, $E \leq E_m \sim 0.1 \cdot E_a$, and b) there are two different ionization regions, one with the electric field ionization and another one with the electron impact ionization. The width of second one is still given by $\Delta_{e-ion} \sim V_f/v_{eI}$, while the width of the first one, $\Delta_{E-ion} = x_m$, can be found from the Poisson equation $E_m/\Delta_{E-ion} \sim 4\pi e n_b$. For the beam energy balance we have $eE_m(\Delta_{E-ion} + \Delta_{e-ion}) \sim W_b$, which gives

$$V_f \sim (1 - E_m^2/4\pi W_b n_b)(W_b v_{eI}/eE_m). \quad (8)$$

The results of the numerical solution of Eq. (5) for $N_a = 3 \cdot 10^{22} \text{ cm}^{-3}$, $K_{bI} = 10^{-10} \text{ cm}^3/\text{s}$, $K_{eI} = 10^{-9} \text{ cm}^3/\text{s}$, and $K_e = 10^{-7} \text{ cm}^3/\text{s}$ (shown in Fig. 1, 2) support our analytic analysis.

IV. Stability of the ionization front. First we consider the stability of the ionization front of width $\Delta_f \sim \Lambda V_f/v_{eI}$ ($L \sim 3$) against long wavelength λ_c corrugation perturbation, $\Delta_f/\lambda_c < 1$. For a small corrugation amplitude, h_c ($\xi_c \equiv h_c k_c \equiv h_c 2\pi/\lambda_c \ll 1$), corrugated ionization front, $X_f(y) = h_c \cos(k_c y)$ does not change much its internal structure in

comparison to 1D case. Therefore local velocity of the ionization front will be determined by local beam parameters. However, due to the effect of the electric field in the front, which slows beam electron and turns them back the local beam density will be altered. The “valleys” of the corrugated front seen by incoming beam electrons will work like focusing lenses and causing a local increase of the beam density, $\delta n_b/n_b \sim \xi_c$, while the “hills” will work other way around. In some sense this focusing works similar to the collimation of the electron beam by vacuum gap observed in numerical modeling in [5]. Notice that the impact of corrugation on the normal (to the front surface) component of beam energy has in the first order approximation over small parameter $\xi_c \ll 1$ can be neglected since $\delta W_b/W_b \sim \xi_c^2 \ll \delta n_b/n_b$. As a result of local variation of beam density the local velocity of the front will be different and will cause the corrugation instability of the front for the case where V_f increases with increasing beam density. To make the quantitative estimate of the growth rate, Γ_c , of such corrugation instability we notice that the diversion of the beam along y-coordinate, δY_b , caused by the electric field effects during beam propagation through the front can be estimated as follows $\delta Y_b \approx \Delta_f (dX_f(y)/dy)$. Therefore the variation of the beam density due to such diversion and corresponding departure of the front velocity from the unperturbed value are $\delta n_b/n_b \approx -d(\delta Y_b)/dy$, $\delta V_f/V_f = (\delta n_b/n_b)(\partial \ln V_f / \partial \ln n_b)$. As a result we find the equation for $X_f(y)$ showing the instability for $(\partial \ln V_f / \partial \ln n_b) > 0$ with the growth rate Γ_c

$$\partial X_f / \partial t = -\Delta_f V_f (\partial \ln V_f / \partial \ln n_b) (\partial^2 X_f / \partial y^2), \quad \Gamma_c = \Delta_f V_f k_c^2 (\partial \ln V_f / \partial \ln n_b) \lesssim v_{eI} / \Lambda. \quad (9)$$

For $N_a = 3 \cdot 10^{22} \text{ cm}^{-3}$, $K_{eI} = 10^{-9} \text{ cm}^3/\text{s}$, and $\Lambda \sim 3$ from (9) we find $\max(\Gamma_c) \sim 10^{13} \text{ s}^{-1}$. Thus for $V_f \sim 10^{10} \text{ cm/s}$, the impact of the corrugation instability on the beam propagation will start to be seen at the distance \sim few tens microns from the front boundary of the insulator.

Next we consider a small-scale (λ_{EI}) electric field ionization instability such that $2\pi\Delta_f/\lambda_{EI} \equiv \Delta_f k_{EI} \gg 1$, but $\delta x_{EI} k_{EI} < 1$. To address this instability we linearize Eq. (1-3) and using both Maxwell and Poisson equations, assuming that the electric field ionization is dominant, the growth rate $\Gamma_{EI} \sim V_f/\delta x_{EI}$ and neglecting small beam density perturbation and keeping only highest order terms in the vicinity of x_m after some algebra we find

$$d\tilde{n}_i/dx + (\Gamma_{EI}/V_f)\tilde{n}_i = -(\sqrt{\pi}U(x)/\delta x_{EI})(\tilde{E}_x/2\pi e), \quad d\delta\tilde{n}/dx + (\Gamma_{EI}/V_f)\delta\tilde{n} + (d\tilde{n}_i/dx) = 0, \\ d^2\tilde{E}_x/dx^2 - (k_{EI}^2 + \Gamma_{EI}^2/c^2)\tilde{E}_x = 4\pi e(d\tilde{n}_i/dx - (\Gamma_{EI}V_f/c^2)\tilde{n}_i) + (4\pi e\Gamma_{EI}/\gamma_f^2 V_f)\delta\tilde{n}, \quad (10)$$

where $U(x) = \exp(-(x - x_m)^2/(\delta x_{EI})^2)/\delta x_{EI}\sqrt{\pi}$, $\tilde{n}_i = (V_E/V_f)\tilde{n}_i$, and $\tilde{n}_i \delta\tilde{n}$, and \tilde{E}_x are the perturbations of the ions density, $\delta n \equiv n_i - n_e$, and the x-component of the electric field strength respectively. For $\delta x_{EI} k_{EI} < 1$ $\tilde{n}_i(x)$, $\delta\tilde{n}(x)$, and $\tilde{E}_x(x)$ vary slowly on the scale $\sim \delta x_{EI}$, so that the function $U(x)$ can be treated as a delta-function. Then, we solve (10) and find the growth rate Γ_{EI}

$$\Gamma_{EI} = \pi^{1/6} \{k_{EI}\delta x_{EI}/(c/V_f + 1)\}^{2/3} (c/\delta x_{EI}) \lesssim v_{eI} (4\pi W_b \bar{n}_b / \epsilon_m^2 E_a^2). \quad (11)$$

In the regimes where the electric field ionization is important, the ratio $4\pi W_b \bar{n}_b / (\epsilon_m^2 E_a^2)$ is large. Therefore comparing expressions (9) and (11) we conclude that the growth rate of small-scale electric field ionization instability is somewhat larger ($\Gamma_{EI} \sim \text{few} \times 10^{13} \text{ s}^{-1}$) than that of large-scale corrugation instability.

V. Conclusions. We consider the structure and stability of the ionization front, which occurs as a high intensity electron beam propagates through an insulator. We show that for relatively small beam energy density $n_b W_b$, the electric field strength in the ionization

region increases with increasing $n_b W_b$. However, when the electric field reaches the value $\sim 0.1 \cdot E_a$ it almost saturates and has very weak logarithmic dependence on the beam parameters. The saturation is caused by the beam charge neutralization due to the electric field ionization processes. We also find that, due to the electric field ionization, the velocity of the front V_f has a non-monotonic dependence on the beam density n_b and in some particular beam density range V_f increases with increasing n_b . We found two instabilities associated with the electric field ionization process of the insulator: a long wavelength (\gtrsim few μ) and relatively slow ($\Gamma_c \sim 10^{13} \text{ s}^{-1}$) corrugation instability and a short wavelength (\sim sub μ) and relatively fast ($\Gamma_{EI} \sim \text{few} \times 10^{13} \text{ s}^{-1}$) electric field ionization instability. The nonlinear stage of the corrugation instability can cause the electrostatic focusing of the electron beam in a manner similar to that observed in the modeling [6], where an impact of the vacuum gap was investigated. Therefore, it is conceivable that the jets and filaments, seen in [2, 3], are the results of nonlinear stage of the ionization front corrugation instability. Comparison of the theoretical estimates of the dynamics of the filament formation, based on the linear growth rate and the front propagation velocity, with the experimental data from [3] shows reasonable agreement.

References

[1] M.H. Key et al., 17th IAEA, Yokohama, 1998, IAEA-CN-69-IF/5; K. Krushelnik, et al., Phys. Plasmas 7 (2000) 2055; S. P. Hatchett, et al., PoP 7 (2000) 2076; R. A. Snavely, et al., PRL 85 (2000) 2945; A. J. MacKinnon, et al., PRL 86 (2001) 1769; M. Borghesi, et al., PRL 92 (2004) 055003; T. E. Cowan, et al., PRL 93 (2004) 204801
 [2] L. Gremillet, et al., PRL 83 (1999) 5015; J. Fuchs, et al., PRL 91 (2003) 255002-1
 [3] R. B. Stephens, et al., Phys. Rev. E 69 (2004) 066414
 [4] V. T. Tikhonchuk, PoP 9 (2002) 1418; D. Batani, et al., Phys. Rev. E 65 (2002) 066409; A. J. Kemp, et al., PoP 11 (2004) 5648, L69
 [5] S. I. Krasheninnikov, A. V. Kim, B. K. Frolov, and R. B. Stephens, PoP (2005) July
 [6] R. B. Campbell, et al., PoP 10 (2003) 4169

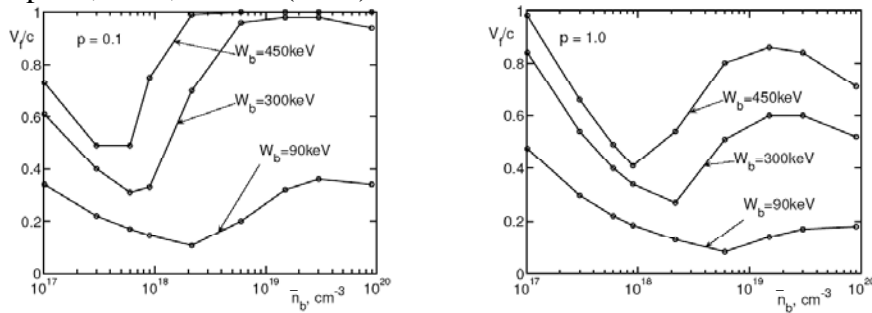


Fig. 1. The front velocity V_f versus beam density \bar{n}_b for different p and W_b

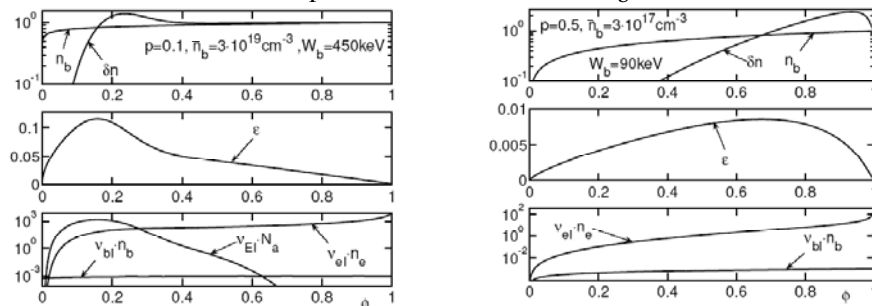


Fig. 2. The profiles of n_b , $\delta n \equiv n_i - n_e$, ϵ , and the ionization sources along ϕ for high and low beam energy densities, where the electric field ionization is- and is not- important